ECS Transactions, 19 (5) 41-52 (2009)
10.1149/1.3119526 ©The Electrochemical Society

Synthesis, Characterization, and Properties of Large-Area Graphene Films

Xuesong Li[a], Weiwei Cai[a], Inhwa Jung[a], Jinho An[a], Dongxing Yang[a], Aruna Velamakanni[a], Richard Piner[a], Luigi Colombo[b], Rodney S. Ruoff[a]

[a] Department of Mechanical Engineering and the Texas Materials Institute, the University of Texas at Austin, Austin, TX 78712
[b] Texas Instruments Incorporated, Dallas, TX 75243

Graphene and few-layer graphene films exhibit unique properties and show promise as electronic devices as well as for passive applications. A significant challenge however is the synthesis of large area graphene and/or multilayer films. A method that is showing promise is the growth of graphene on metal substrates by chemical vapor deposition. In this paper we report on a method to grow large-area graphene films on Cu foils and graphene transfer methods to other substrates. The transferred graphene films were characterized by optical, scanning and transmission electron microscopy, Raman and UV-VIS spectroscopy, and four-point probe electrical measurements. The data shows that graphene can be grown directly on Cu substrates by chemical vapor deposition. The graphene films transferred to SiO_2/Si substrates show low defects as determined by the near absence of the "D" band at 1350 cm^{-1} in the Raman spectrum. In addition, the films were found to have high optical transmittance and electrical conductivity.

1. Introduction

Graphene, a monolayer of sp^2-bonded carbon atoms, is a quasi-2-dimensional (2D) material.(*1*) Graphene and few layer graphene (FLG) possess unique transport properties and this makes them of interest for new electronic devices.(*1-10*) Graphene-based films with sufficiently high transmittance and electrical conductivity can also be considered for applications requiring optically transparent conductors,(*11-15*) perhaps as a replacement of the traditional thin metallic or metal oxide films such as indium tin oxide (ITO).

In order for graphene to be useful for practical applications it is important to produce it in large areas. To date, the primary method for making graphene is by micromechanical cleavage of graphite,(*1*) which can only produce very small graphene films. It has been recently stated that graphene can be produced by exfoliation and dispersion of graphite in certain organic solvents, but the yield is very low and large area films are not continuous.(*13, 16*) The chemical reduction of exfoliated graphite oxide may be a candidate for large-scale preparation of graphene.(*17-22*) However, it might be difficult to fully recover the electrical properties of graphene from oxidized graphene sheets. Another promising method is to grow graphene or FLG directly via vacuum graphitization of silicon carbide substrates, (*23, 24*). However, graphene grown on SiC substrates may be difficult to transfer to other substrates, such as silicon, for integration with Si based devices.

Thick graphite films have been formed by segregation of carbon from carbon-saturated metals such as Ni and Fe. This is a well established process in Fe but the solubility of carbon in Fe and Ni is high and thus these are good metals for the synthesis of thick graphite films. The thickness of the graphite layers is determined by the amount of segregated C, which can be controlled by the temperature of the metal-carbon solution and the thickness of the metal substrate. For example, C has a "high" solubility in Ni (*25*) and a 50-μm thick Ni foil (saturated with C at ~ 1000 ^{o}C) can produce graphite with a thickness of several microns.(*26*) This segregation mechanism was also proposed for the case of graphene grown on metal substrates: by decreasing the thickness of the Ni film to tens to hundreds of nanometers, or by cooling the C/Ni alloy quickly, FLG films can be achieved.(*27-29*) However, it should be noted that an abrupt formation of a monolayer graphene on single crystal Ni was observed at the temperature higher than the carbon precipitation temperature. (*30, 31*) This suggests that for the case of FLG growth presented here, another mechanism may be important. A detailed explanation of the growth mechanism is beyond the scope of this work as further work is indicated.

In this work we report on a method to grow large-area graphene films on Cu foils. There are a few reasons for the selection of Cu metal as a substrate: 1) the Cu/C binary phase diagram shows a low carbon solubility (*32*) which limits the amount of segregated C and hence can lead to better control of graphene film growth over a reasonable temperature range (800-1000^{o}C), 2) absence of a copper carbide line compound, and 3) wet etchant selectivity to graphene. In this paper we also report on a few methods to transfer the graphene films from the Cu metal surface to substrates such as SiO_2/Si, glass, or flexible polydimethylsiloxane (PDMS). Our method may provide a pathway to controlled scalable production of graphene and thus large-scale fabrication of graphene devices.

2. Experimental

2.1 Graphene Synthesis

A horizontal tube furnace with a 22-mm ID fused silica tube was used to synthesize graphene films. Twenty-five micron thick Cu foils with a 99.8% purity purchased from Alfa Aesar were used as the metal substrate. Methane (Air Gas Inc. ultra high purity grade) was used as the carbon source and hydrogen (Air Gas Inc. ultra high purity grade) was used to clean the copper surface of any unwanted oxide or physisorbed species before growth. A typical process flow chart and temperature profile is shown in Fig. 1 a & b, respectively.

Methane (ultra high purity grade) was used as the carbon source and hydrogen (ultra high purity grade) was used to clean the copper surface of any unwanted oxide or physisorbed species before growth. The process flow for a typical growth run is shown below.

2.2 Graphene Transfer

Graphene films were removed from the Cu foils by wet etching Cu with an aqueous solution of iron nitrate and water. The etching time is a function of the etchant concentration and the amount of Cu. Typically, the Cu foil (25-μm in thickness and 1 by

1 cm^2 in area) was found to be fully dissolved by 0.05 g/ml iron nitrate solution over night.

- 25 mm thick 99.8% pure Cu foil
- Load Cu foil in furnace
- Evacuate furnace to P < 40 mTorr
- Backfill with H_2 to a P = 400 mTorr and flow at 100 sccm
- Heat to T = 900 °C under H_2
- Anneal at T = 900 °C for 30 min
- Introduce methane at a flow rate of 30 sccm and P = 400 mTorr
- Flow methane at T = 900 °C for 30 min
- Decrease methane flow to 12 sccm
- Shut off furnace and cool to room temperature
- Shut off methane and evacuate
- Backfill with nitrogen to 1 atm
- Unload Cu/ graphene foil

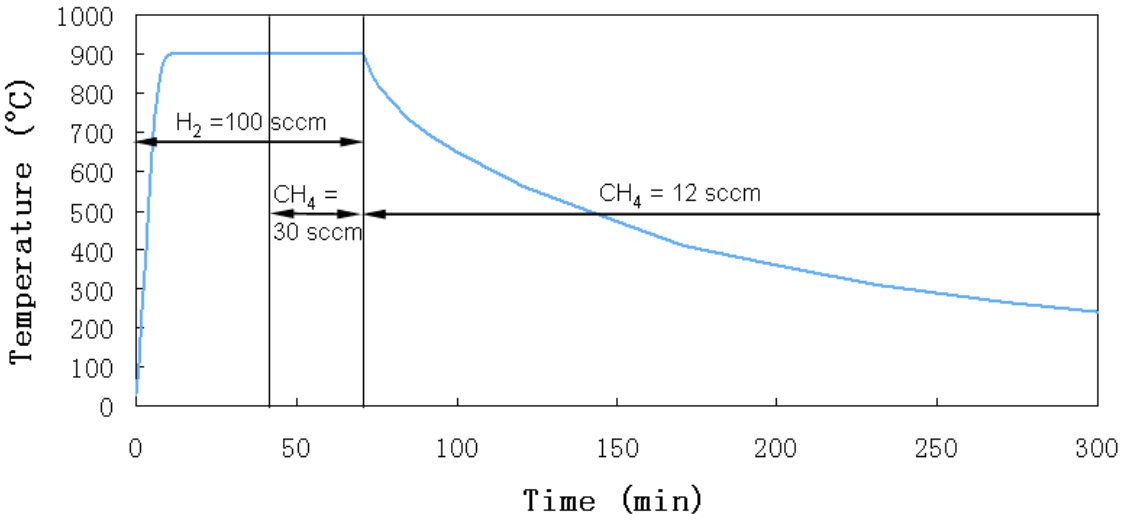

Figure 1. Graphene synthesis process flow and the temperature profiles.

Since both copper surfaces are exposed to methane graphene was found on both sides of the Cu foil. As a result, care must be taken in isolating the two films in order to prevent them from collapsing on each other upon dissolution of the copper foil. To avoid this a thin metal film, Au, was deposited on one side of the Cu foil to help it precipitate to the bottom of the container. The floating film could then be removed from the solution in a number of ways: 1) tweezers (in this case, the film shrunk into a "rope"), 2) by bringing another substrate in contact with the film directly at the liquid surface, 3) by coating the graphene-on-Cu with a thin layer of polydimethylsiloxane (PDMS) which does not react with the iron nitrate solution, followed by removal from the solution after complete etching of the Cu foil. These schemes are shown in Fig. 2. The graphene films were washed to remove salt residues in two separate ways: (a) dilution of the etchant solution multiple times by high purity water while the FLG film was still floating on the liquid surface; (b) washing the transferred films with high purity water directly (the adhesion between the graphene film and the substrate is evidently strong enough that it is not washed off).

2.3 Characterization

Optical microscopy and Raman spectroscopy (WITec alpha300 with a laser wavelength of 532 nm), scanning electron microscopy (SEM; FEI Quanta-600), and Transmission electron microscopy (TEM, JEOL 2010F) were used to characterize the graphene films. A spectroscopic ellipsometer (JA Woolam, M-2000) was used for the measurement of the transmittance of the graphene films.

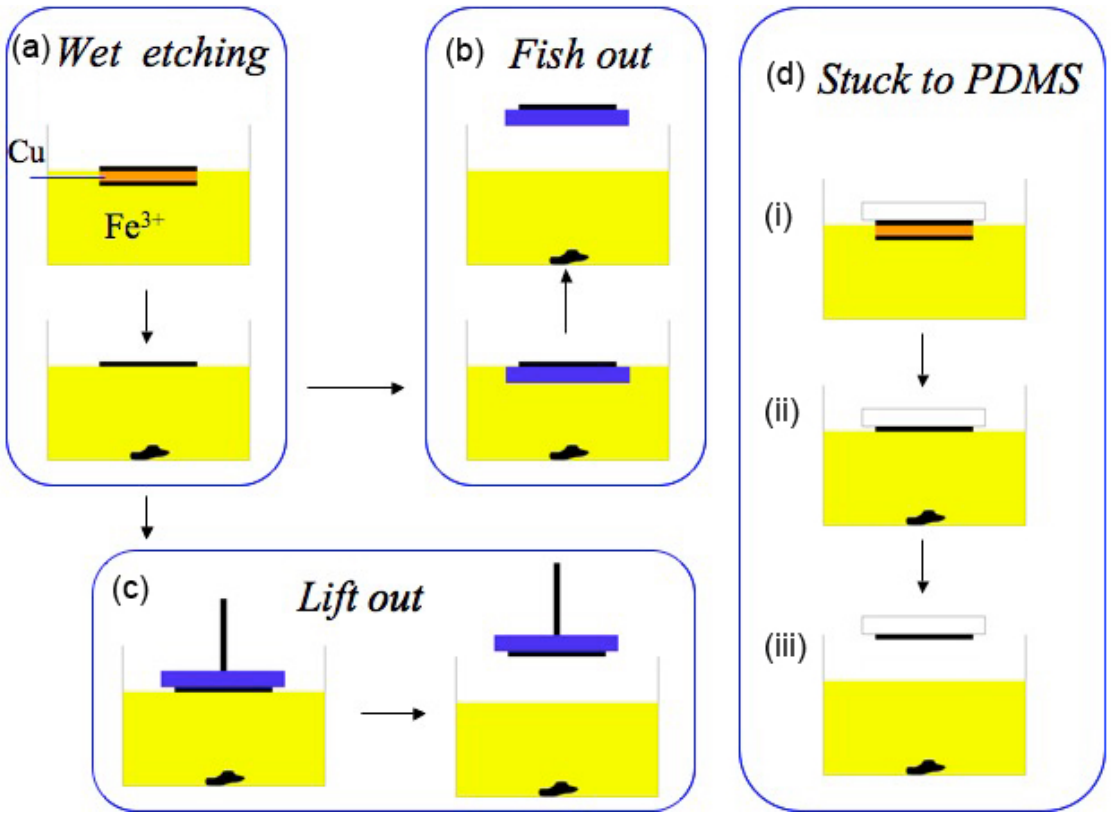

Figure 2. Schematic representation of wet etching of Cu foil (a) and transfer of the floating few-layer graphene (FLG) film by "fishing out" (b), or lifting out (c). (d) The Cu foil with a FLG film was coated with a thin film of PDMS before etching (i); after Cu was fully dissolved, a FLG film was left onto the PDMS film (ii) and (iii).

The electrical conductivity of these graphene films was measured by the van der Pauw method. (*33, 34*) The graphene films were 1 cm by 1 cm squares and the 4 electrodes (Cu wires) were connected to the 4 corners of the film with silver paint (Fig.3). Four different configurations are possible by rotating the current source and the positions of the voltage measurement. For example, in the configuration 1, current flow was applied between the points 1 and 2 and the voltage drop was measured between the points 4 and 3. The resistance in this configuration can be calculated by Ohm's law as follows:

$$R_{12,43} = V_{43} / I_{12} \quad (1)$$

$$V_{43} = V_1 - V_2 \quad (2)$$

In the same way, resistance can be measured at each configuration. Sheet resistances are determined by averaging four resistance values from these configurations.

$$R_{sheet} = \pi/\ln(2)\, f\, (R_{12,43} + R_{14,23} + R_{43,12} + R_{23,14})/4 \quad (3)$$

The correction factor (f) is determined from the ratio of resistances taken in orthogonal directions.

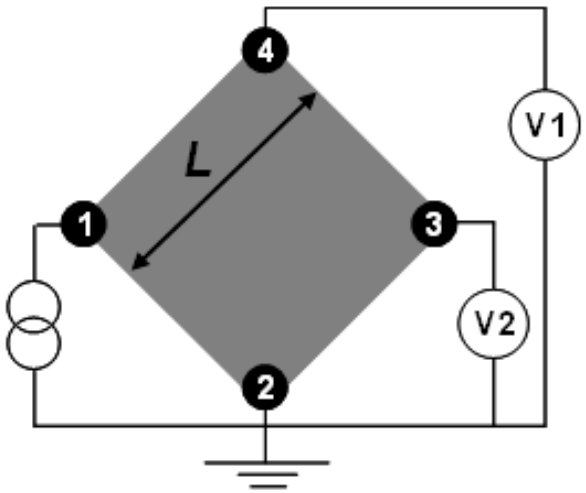

Figure 3. Four probe configuration for measuring conductivity of FLG film.

3. Results and Discussions

3.1 Physical Characterization

Figure 4a shows a 1 cm by 1 cm graphene film floating on water, which was then transferred onto a 1.8 cm by 1.8 cm cover glass (Fig. 4b). Fig. 4c shows a 1.8 cm by 1.8 cm graphene film on PDMS, transferred by the method schematically shown in Fig. 2d. Because the graphene film is the same size as the copper substrate the lateral size of the graphene can be easily scaled to any much larger size.

Figs. 4d &e show a graphene "rope" picked up from the echant solution by tweezers. The graphene film is continuous and it seems to be strong. Further characterization on the mechanical properties of the graphene film will be reported in the future.

Transmission electron microscopy (TEM) was also performed to evaluate the number of graphene layers and to assess the crystalline quality of the graphene films. Fig. 5a shows a TEM image of the graphene film transferred from a Cu foil onto a TEM grid with the circled area marking the location where an electron diffraction pattern was obtained (Fig. 5b). The electron diffraction pattern shows that the film has a graphite-like hexagonal structure. The number of layers of graphene in these different pieces of this film was identified by counting the number of fringes at the edges of the sample. The fringes are a result of folded layers at the edges of the transferred film.(*3*). The number of layers of graphene in the film is 2 to 3 layers (Fig. 5c).

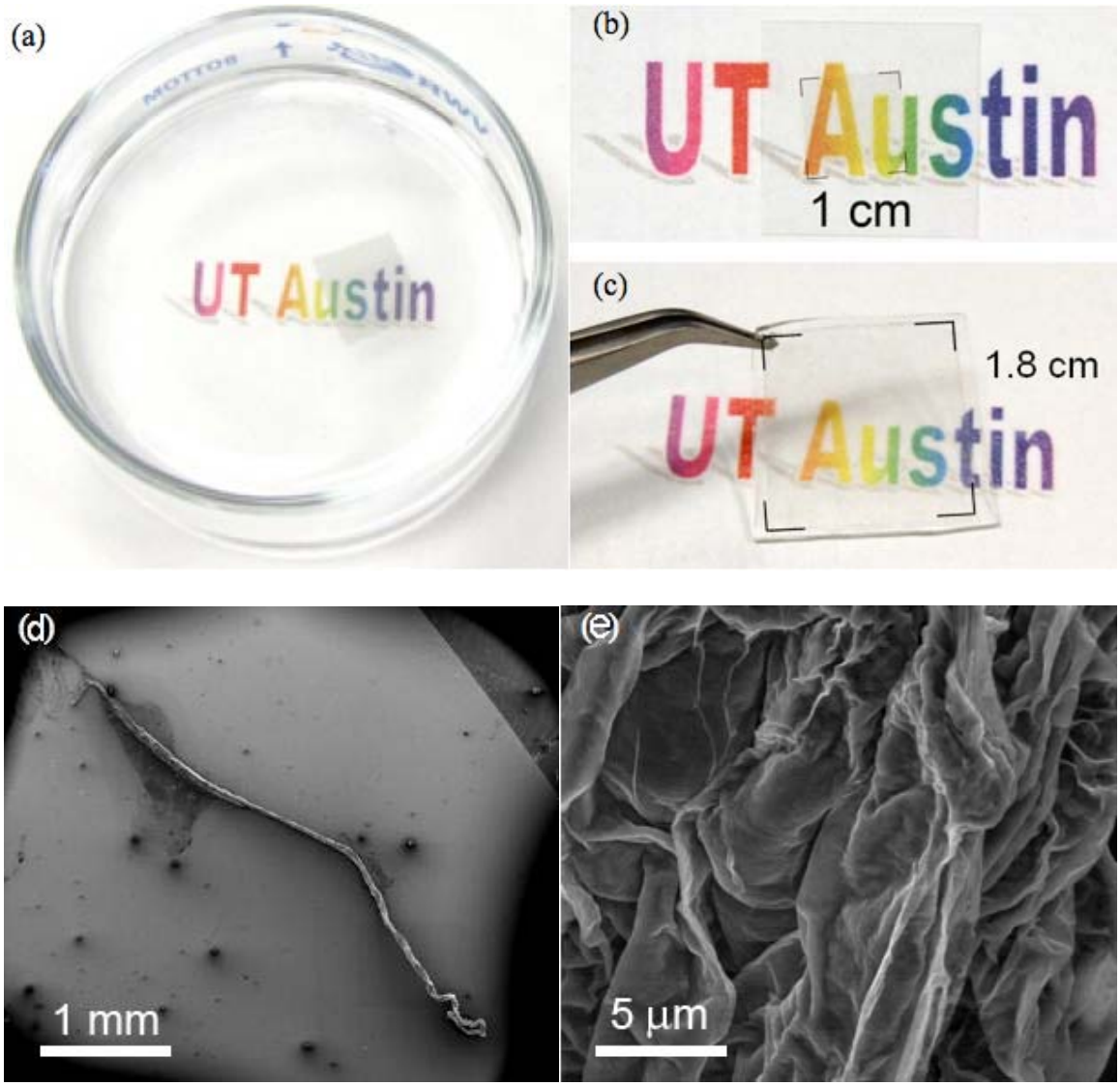

Figure 4. (a) A 1 cm by 1 cm transparent graphene film floating on water. (b) A 1 cm by 1 cm graphene film transferred on a 1.8 cm by 1.8 cm cover glass. (c) A 1.8 cm by 1.8 cm graphene film stuck on a PDMS film. Rolled up graphene "rope" in low (d) and high (e) magnification, respectively.

Figure 6 shows an optical micrograph and Raman spectra of the graphene film transferred onto the SiO_2/Si substrate. In contrast to the FLG grown on Ni film, which has a large distribution of layers, from 1 to several tens,(*28*) the layers transferred from Cu are thinner and much more uniform as shown by Fig. 6a. Fig 6a shows a graphene film transferred onto a SiO_2/Si substrate with the edge shown at the top of the image. The low color contrast between the graphene film and the substrate suggests that the number of graphene layers is uniform.(*35*)

The crystal quality of FLG films can be characterized by Raman spectroscopy.(*36*) Fig. 6b shows typical Raman spectra of HOPG, monolayer graphene, and FLG films transferred on Si/SiO_2 (285 nm) substrates from the Cu foils. The spectrum shows two main bands marked as G and 2D. A third band referred to as the D band found at ~ 1350 cm^{-1} that is usually associated with defects in the graphene is not present in these films

suggesting that the initial film quality is as good as that of HOPG as determined by Raman spectroscopy.

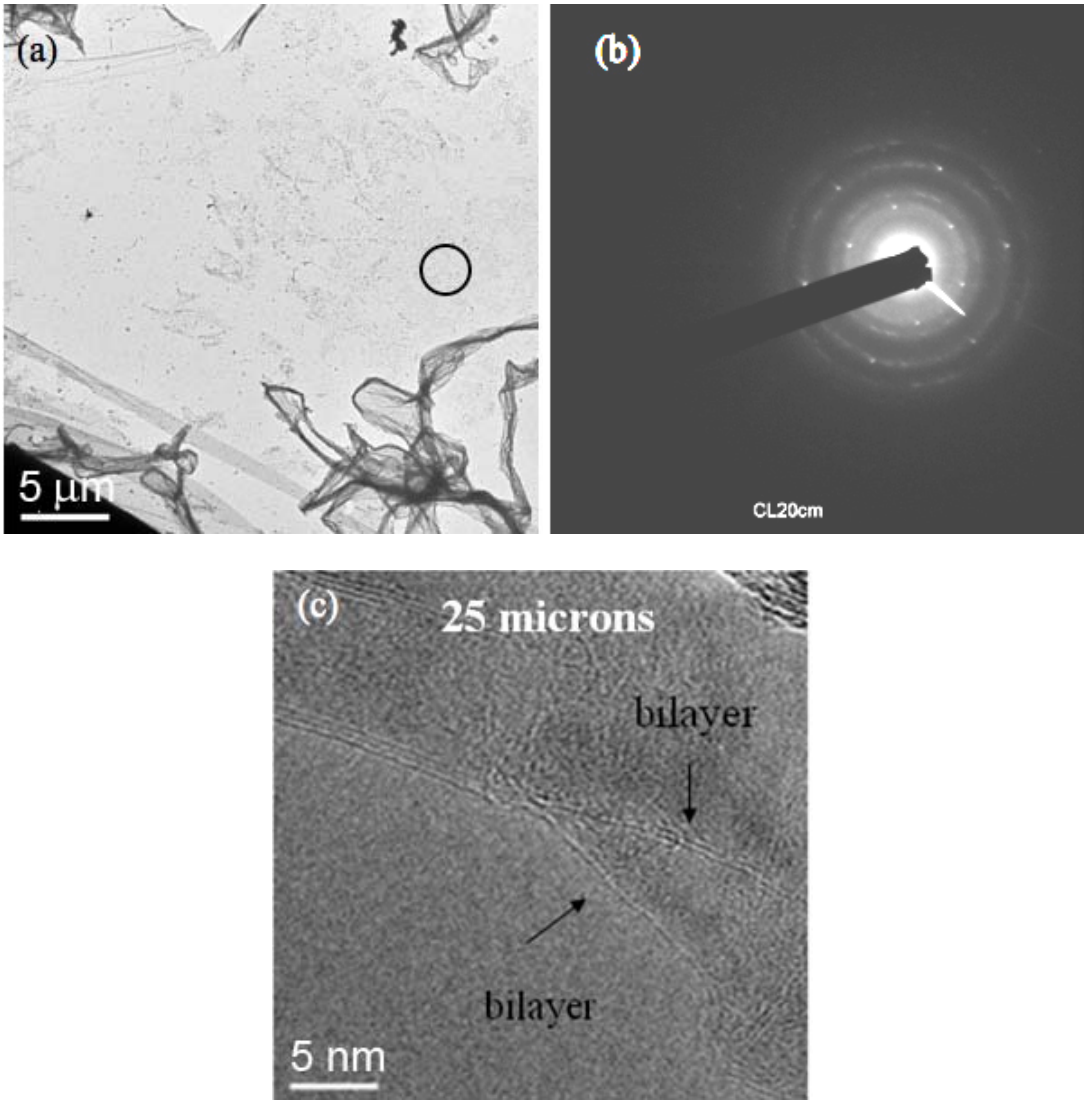

Figure 5. TEM images of graphene films. (a) Low magnification image of graphene film on TEM grid and (b) electron diffraction pattern from circled area in (a). (c) 2- and 3-layer graphene transferred from 25-μm thick Cu foil.

Raman spectroscopy can also be used to characterize the number of stacked graphene layers using the position and shape of the 2*D* band around 2700 cm^{-1}.(*28, 35, 37, 38*) The 2*D* band of monolayer graphene at 2678.8±1.0 cm^{-1} is sharp and symmetric,(*38*) and distinguishable from those of FLG and bulk graphite. The Raman spectra in Figure 6b clearly show the differences between the three different materials HOPG, FLG, and graphene. The G band of HOPG shows the expected features and the G-bands of graphene and FLG have the same shape and differ only in intensity also as expected. We measured many spots across the as-grown carbon films on Cu by Raman spectroscopy and found that the films are predominantly graphene, over 90% of the area, i.e., single layer graphite.

Fig. 7a shows the as-grown graphene film on Cu foil with the presence of wrinkles. The wrinkles are associated with the thermal expansion coefficient difference between Cu and graphene. It can be seen that the wrinkles span the grain boundaries, indicating that graphene grows across the grain boundaries. The SEM image of a graphene film transferred onto a SiO_2/Si wafer in Fig. 7b further shows that the film is macroscopically continuous and uniform over square millimeters.

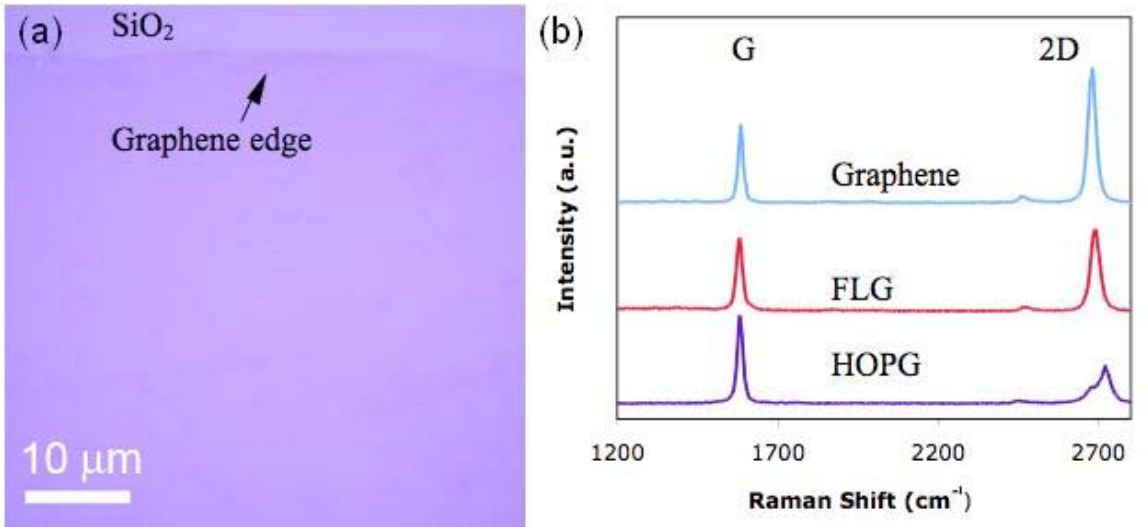

Figure 6. (a) Optical micrograph of graphene film transferred from 25-μm Cu onto a piece of Si wafer with a 285-nm SiO_2 layer. (b) Raman spectra of graphene films, taken from regions with different thicknesses. HOPG was used as a control.

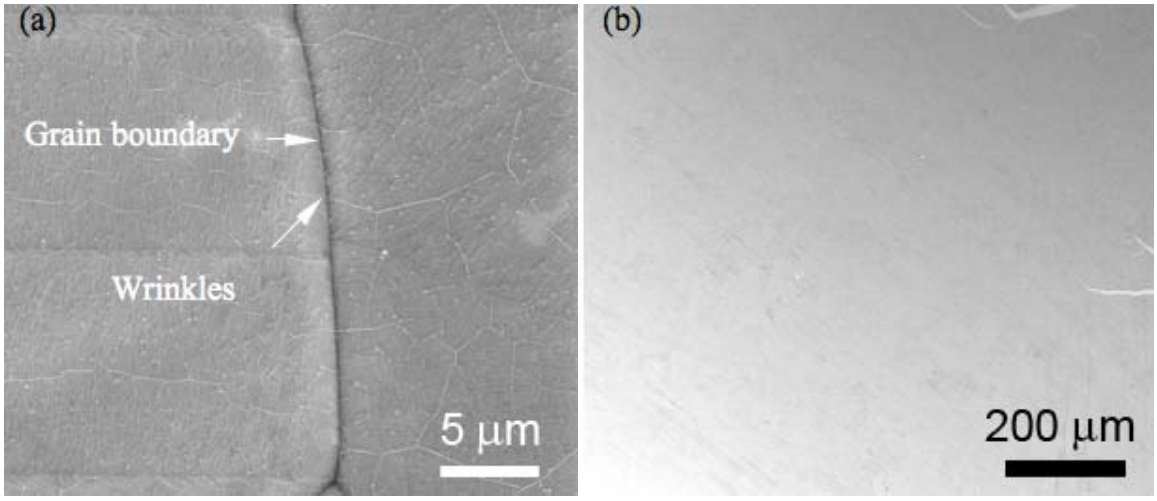

Figure 7. Graphene film on (a) Cu foil and (b) transferred to SiO_2/Si wafer.

3.2 Optical Transmittance and Electrical Conductivity of Graphene

We also measured the optical transmittance and sheet resistance of the graphene films as shown Fig. 9a where the transmittance at 550-nm wavelength is 0.97. It has been reported that the transmittance of graphene at 550 nm is 97.7%.(*11*) The sheet resistance of the same film is 1.3×10^4 to 5.1×10^4 Ω/sq. From these data, the thickness of the graphene film can be estimated to be 0.44 nm assuming that the attenuation coefficient is

the same as a graphene and the calculated average conductivity for the film is 0.7×10^5 S/m. The lower conductivity of the thin film may result from some tearing of the film created during the transfer process.

Table 1 shows the conductivity of our graphene films compared to films prepared by other techniques, and graphite. It can be seen that the conductivity of our graphene film is comparable to that of "high temperature" pyrolytic carbon, but lower than that of HOPG and natural graphite by one order of magnitude. The conductivity of our graphene films are higher than that of films deposited from colloidal suspensions that are composed of reduced graphene oxide platelets.

TABLE I. Conductivity of graphene films and graphite[a]

Materials	Conductivity ($\times10^5$ S/m)	Refs.
Graphene (CVD on Cu)	0.7	this work
Spray-coated graphene film	1.3	(*13*)
Reduced graphene oxide	0.55	(*12*)
	0.35	(*21*)
Pyrolytic carbon[b]	2	(*39*)
HOPG	22 to 28	(*39, 40*)
Natural graphite	25	(*41*)

[a]In-plane (a-Axis) conductivity for graphite and pyrolytic carbon are listed.
[b]Deposition temperature 2100 to 2200 °C.

Figure 8b shows the comparison of transmittance (at 550 nm wavelength) and sheet resistance of our graphene films with those of other graphene/graphene oxide films reported to date, to single-walled carbon nanotube (SWCNT) films, and indium tin oxide (ITO). The graphene films grown on Cu have a good combination of high transmittance and low resistance that could make FLG an attractive replacement for ITO if process improvements and production issues can be addressed.

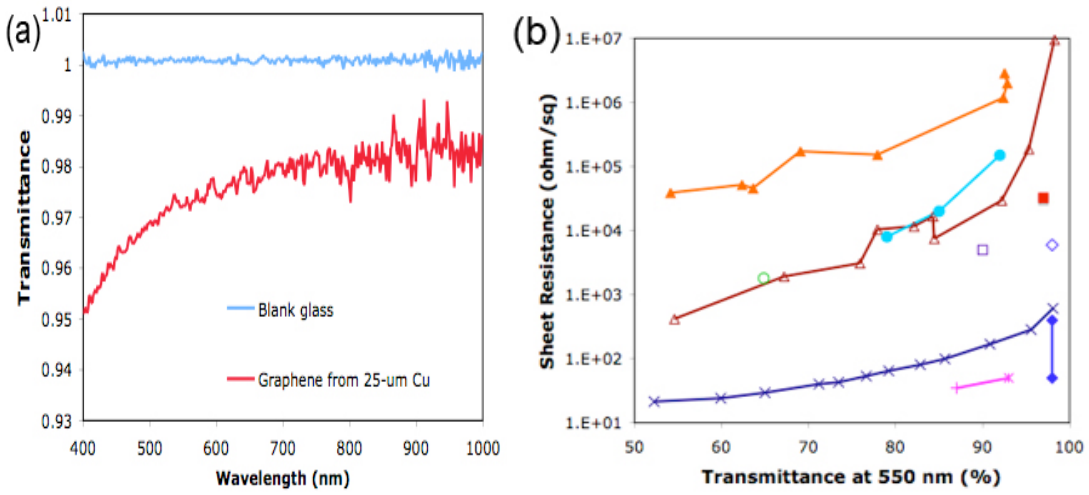

Figure 8. (a) The transmittance of FLG films from 400-1000 nm. The transmittance at 550-nm is 0.97 for thin graphene film and 0.91 for thick one, respectively. (b) Plots of sheet resistance vs transmittance at 550 nm, in comparison with other transparent conductive films: ■ FLG film (this work), ▲(*15*) graphene oxide treated with hydrazine vapor plus annealing at 400 °C, △(*15*) & ○(*12*) graphene oxide film graphitized at 1100 °C, ●(*14*) Langmuir-Blodgett film of graphene sheets, □(*13*) spray-coated graphene film,

◇(*2*) undoped monolayer graphene, ◆(*1, 5, 13*) doped monolayer graphene, ×(*42*) single-walled carbon nanotube film, +(*43*) & ∗(*44*) indium tin oxide.

Although the sheet resistance of graphene films fabricated so far is higher than that of traditional transparent conductors such as ITO, graphene films may have advantages, such as high chemical stability and mechanical strength.(*12, 13*) SWCNT films have exhibited high optical transmittance and low sheet resistance.(*42*) However, SWCNT films are a network of nanotubes with gaps and thus will not have good barrier properties if this is important in certain applications. While the sheet resistance of our graphene is still too high, Fig 8b, with respect to the theoretically expected values we believe that further improvements will yield lower sheet resistance.

4. Conclusions

Large-area graphene films were synthesized on Cu foils. The as-grown graphene was transferred to other substrates by wet chemical etching of the Cu. The transferred graphene films have good crystalline quality as determined by TEM and Raman spectroscopy. The optical transmittance and electrical conductivity values of these films suggest potential applications in optoelectronics. This method of synthesizing graphene is scalable to very large substrates and is thus potentially compatible with sizes required by the semiconductor industry. Further material growth optimization is needed to achieve precise mono layer growth in order to meet the very stringent semiconductor device requirements.

Acknowledgments

We would like to thank the Nanoelectronic Research Initiative (NRI-SWAN; #2006-NE-1464) and The University of Texas at Austin for support of this work.

References

1. K. S. Novoselov *et al.*, Electric field effect in atomically thin carbon films, *Science* **306**, 666 (2004).
2. A. K. Geim, K. S. Novoselov, The rise of graphene, *Nat. Mater.* **6**, 183 (2007).
3. J. C. Meyer *et al.*, The structure of suspended graphene sheets, *Nature* **446**, 60 (2007).
4. J. S. Bunch *et al.*, Electromechanical resonators from graphene sheets, *Science* **315**, 490 (2007).
5. F. Schedin *et al.*, Detection of individual gas molecules adsorbed on graphene, *Nat. Mater.* **6**, 652 (2007).
6. H. B. Heersche, P. Jarillo-Herrero, J. B. Oostinga, L. M. K. Vandersypen, A. F. Morpurgo, Bipolar supercurrent in graphene, *Nature* **446**, 56 (2007).
7. K. S. Novoselov *et al.*, Unconventional quantum Hall effect and Berry's phase of 2π in bilayer graphene, *Nature Physics* **2**, 177 (2006).
8. Y. Zhang, J. P. Small, W. V. Pontius, P. Kim, Fabrication and eletric-field-dependent transport measurements of mesoscopic graphite devices, *Appl. Phys. Lett.* **86**, 073104 (2005).

9. C. Berger *et al.*, Ultrathin epitaxial graphite: 2D electron gas properties and a route toward graphene-based nanoelectronics, *J. Phys. Chem. B* **108**, 19912 (2004).
10. J. S. Bunch, Y. Yaish, M. Brink, K. Bolotin, P. L. Mceuen, Coulomb oscillations and hall effect in quasi-2D graphite quantum dots, *Nano Letters* **5**, 287 (2005).
11. R. R. Nair *et al.*, Fine structure constant defines visual transparency of graphene, *Science* **320**, 1308 (2008).
12. X. Wang, L. Zhi, K. Müllen, Transparent, conductive graphene electrodes for dye-sensitized solar cells, *Nano Letters* **8**, 323 (2008).
13. P. Blake *et al.*, Graphene-based liquid crystal device, *Nano Letters* **8**, 1704 (2008).
14. X. Li *et al.*, Highly conducting graphene sheets and Langmuir-Blodgett films, *Nature Nanotechnology* **3**, 538 (2008).
15. H. A. Becerril *et al.*, Evaluation of solution-processed reduce graphene oxide films as transparent conductors, *ACS Nano* **2**, 463 (2008).
16. Y. Hernandez *et al.*, High-yield production of graphene by liquid-phase exfoliation of graphite, *Nature Nanotechnology*, (2008).
17. S. Stankovich *et al.*, Graphene-based composite materials, *Nature* **442**, 282 (2006).
18. S. Stankovich *et al.*, Synthesis of graphene-based nanosheets via chemical reduction of exfoliated graphite oxide, *Carbon* **45**, 1558 (2007).
19. S. Gilje, S. Han, M. Wang, K. L. Wang, R. B. Kaner, A chemical route to graphene for device applications, *Nano Letters* **7**, 3394 (2007).
20. K. N. Kudin *et al.*, Raman spectra of graphite oxide and functionalized graphene sheets, *Nano Letters* **8**, 36 (2008).
21. Y. Y. Wang *et al.*, Raman studies of monolayer graphene: The substrate effect, *J Phys Chem C* **112**, 10637 (2008).
22. Y. Si, E. T. Samulski, Synthesis of water soluble graphene, *Nano Letters* **8**, 1679 (2008).
23. C. Berger *et al.*, Electronic confinement and coherence in patterned epitaxial graphene, *Science* **312**, 1991 (2006).
24. J. Hass *et al.*, Highly ordered graphene for two dimensional electronics, *Appl. Phys. Lett.* **89**, 143106 (2006).
25. J. J. Lander, H. E. Kern, A. L. Beach, Solubility and diffusion coefficent of carbon in nickel: reaction rates of nickel-carbon alloys with barium oxide, *J. Appl. Phys.* **23**, 1305 (1952).
26. W. W. Cai *et al.*, Synthesis and solid-state NMR structural characterization of C-13-labeled graphite oxide, *Science* **321**, 1815 (2008).
27. Q. Yu *et al.*, Graphene segregated on Ni surfaces and transferred to insulators, *Appl. Phys. Lett.* **93**, 113103 (2008).
28. A. Reina *et al.*, Large Area, Few-Layer Graphene Films on Arbitrary Substrates by Chemical Vapor Deposition, *Nano Letters*, ASAP (2008).
29. K. S. Kim *et al.*, Large-scale pattern growth of graphene films for stretchable transparent electrodes, *Nature*, online (2009).
30. M. Eizenberg, J. M. Blakely, Carbon interaction with nickel surfaces - monolayer formation and structural stability, *Journal of Chemical Physics* **71**, 3467 (1979).
31. M. Eizenberg, J. M. Blakely, Carbon monolayer phase condensation on Ni(111), *Surface Science* **82**, 228 (1979).
32. G. A. López, E. J. Mittemeijer, The solubility of C in solid Cu, *Scripta Materialia* **51**, 1 (2004).

33. L. J. Van Der Pauw, *Philips Research Reports* **20**, 220 (1958).
34. L. J. Van Der Pauw, *Philips Research Reports* **13**, 1 (1958).
35. Z. H. Ni *et al.*, Graphene thickness determination using reflection and contrast spectroscopy, *Nano Letters* **7**, 2758 (2007).
36. P. Lespadea, A. Marchanda, M. Couzib, F. Cruege, Caracterisation de materiaux carbones par microspectrometrie Rama, *Carbon* **22**, 375 (1984).
37. A. C. Ferrari *et al.*, Raman spectrum of graphene and graphene layers, *Phys. Rev. Lett.* **97**, 187401 (2006).
38. D. Graf *et al.*, Spatially resolved Raman spectroscopy of single- and few-layer graphene *Nano Letters* **7**, 238 (2007).
39. C. A. Kleim, *J. Appl. Phys.* **33**, 3338 (1962).
40. I. L. Spain, A. R. Ubbelohde, D. A. Young, *Phil. Trans, Roy, Soc. (London)* **262**, 345 (1967).
41. D. E. Soule, *Phys. Rev.* **112**, 698 (1958).
42. H.-Z. Geng *et al.*, Effect of acid treatment on carbon nanotube-base flexible transparent conducting films, *J. Am. Chem, Soc* **129**, 7758 (2007).
43. H. Kim, J. S. Horwitz, G. P. Kushto, Z. H. Kafafi, D. B. Chrisey, Indium tin oxide thin films grown on flexible plastic substrates by pulsed-laser deposition for organic light-emitting diodes, *Appl. Phys. Lett.* **79**, 284 (2001).
44. F. L. Wong, M. K. Fung, S. W. Tong, C. S. Lee, L. S. T, Flexible organic light-emitting device based on magnetron sputter indium-tin-oxide on plastic substrate, *Thin Solid Films* **466**, 225 (2004).